Journal of Crystal Growth 323 (2011) 21–25

Contents lists available at ScienceDirect

Journal of Crystal Growth

journal homepage: www.elsevier.com/locate/jcrysgro

Investigation of metamorphic InGaAs quantum wells using N-incorporated buffer on GaAs grown by MBE

Yuxin Song [a,*], Shumin Wang [a], Xiaohui Cao [a], Zonghe Lai [b], Mahdad Sadeghi [b]

[a] Photonics Laboratory, Department of Microtechnology and Nanoscience, Chalmers University of Technology, SE-41296 Göteborg, Sweden
[b] Nanofabrication Laboratory, Department of Microtechnology and Nanoscience, Chalmers University of Technology, SE-41296 Göteborg, Sweden

ARTICLE INFO

Available online 21 December 2010

Keywords:
A1. Dislocations
A3. Molecular beam epitaxy
A3. Semiconducting III–V materials

ABSTRACT

Strong enhancement of photoluminescence intensity from InGaAs quantum wells by incorporating nitrogen in metamorphic InGaAs buffers grown on GaAs substrates was demonstrated and investigated. The enhancement of photoluminescence intensity is found to be from both the weak strain effect and the strong lattice hardening effect, indicating blocking effect of threading dislocations due to the N incorporation. Combination of this method with a strain compensated superlattice was proved to be effective in obtaining good quality metamorphic InGaAs quantum wells.

1. Introduction

Restricted by the availability of large and high-quality commercial substrates, only a small range of materials with a lattice constant close to certain substrates, such as GaAs and InP, could be used in the design of epitaxially grown devices, otherwise strain relaxation and formation of defects will cause severe problems. With the help of a relaxed metamorphic buffer on top of a standard substrate, one can produce a virtual substrate with a desired lattice constant and obtain strain free devices above it. The metamorphic growth method gives a much larger freedom on the design of heterostructures and has already given rise to commercialized electronic devices, i.e. high electron mobility transistors (HEMTs) [1], and promises to be one of the solutions for electronic and optoelectronic integration on the same substrates [2]. The main challenges of this method are the rough interface and a high density of threading dislocations (TDs) in the active region of the devices [3]. The latter problem is more critical for the optoelectronic devices such as lasers, which have large device areas and therefore are very sensitive to TDs in the active region. Several different metamorphic buffer designs have been implemented to reduce the TD density, e.g., use of a thick uniform buffer layer [4,5], a step-graded buffer layer [6,7] and a continuously graded buffer layer [8–11]. Other structures like strained superlattice (SL) [12] and quantum dots [13] are also employed to block TDs after they have been generated. Although there have been notable progresses for metamorphic optoelectronic devices based on these methods [5,9,14,15], further reduction of the TD density and correspondingly the enhancement of optical quality is still required to improve the device performance and make them competitive with existing products.

Dilute nitrides are well known to reduce the bandgap of many III–V host materials and have been used to fabricate high performance 1.3 μm telecom lasers on GaAs [16,17]. Recently, incorporation of nitrogen has also shown its effect on strain relaxation, dislocation formation and motion in tensile-strained GaAsP [18], which could be helpful for the TD reduction in metamorphic structures. We demonstrated strong improvements in optical quality in metamorphic quantum wells (QWs) by incorporation of dilute nitrides in compressively strained InGaAs grown on GaAs substrates [19]. In this article, we further investigate the effects of dilute nitrogen on TDs and optical quality of metamorphic QWs and evaluate the effectiveness of this method for structures with different In compositions.

2. Experiments and methods

2.1. Sample design, growth and characterizations

All the samples were grown by a VEECO EPI930 molecular beam epitaxy (MBE) system. Two groups of metamorphic InGaAs samples on GaAs substrates were designed. Group I has small lattice mismatch (0.7%) while Group II has large lattice mismatch (2.2%) aiming for 1.55 μm light emission. Fig. 1 shows the schematic structure of the two groups of samples. First, a 100 nm thick GaAs buffer layer was grown at 580 °C measured by a pyrometer to obtain a smooth growth front. The relaxed buffer consists of a 200 nm thick bulk $In_{0.15}Ga_{0.85}As$ and a 500 nm thick bulk $In_{0.31}Ga_{0.89}As$ for Group I and II samples, respectively. On top of the relaxed buffer, a 200 nm thick "TD blocking region" is grown

* Corresponding author.
E-mail address: yuxin.song@chalmers.se (Y. Song).

0022-0248/$ - see front matter © 2010 Elsevier B.V. All rights reserved.
doi:10.1016/j.jcrysgro.2010.12.048

with different schemes described in Table 1. A QW structure (blue shaded area) is grown in all the samples for comparison of optical quality. The QW structure is identical in each group. The 3 nm AlAs layer in the structure acts as a barrier to avoid the excited carriers diffusing out of the QW region, while the thin GaAs layers are used to smoothen the growth front and to protect surface.

The whole structure except the first GaAs buffer layer was grown at 500 °C. Samples were characterized by atomic force microscopy (AFM), transmission electron microscopy (TEM), photoluminescence (PL) and X-ray diffraction (XRD). The AFM measurements were performed using a Veeco Dimension 3000 SPM with a height resolution of 0.1 nm. The XRD measurements were done by a Philips X'Pert Materials Research Diffractometer (MRD). The TEM measurements were performed by a PHILLIPS CM200 TEM system. For the PL measurements, an argon-ion laser (514.5 nm line) was used as the excitation source. The emissions were dispersed by a Spex 1404 0.85 m double grating monochromator and detected with a liquid nitrogen-cooled North-Coast Ge detector. A standard lock-in amplifier was used to detect the signal. All the PL measurement, unless declared, are measured at room temperature.

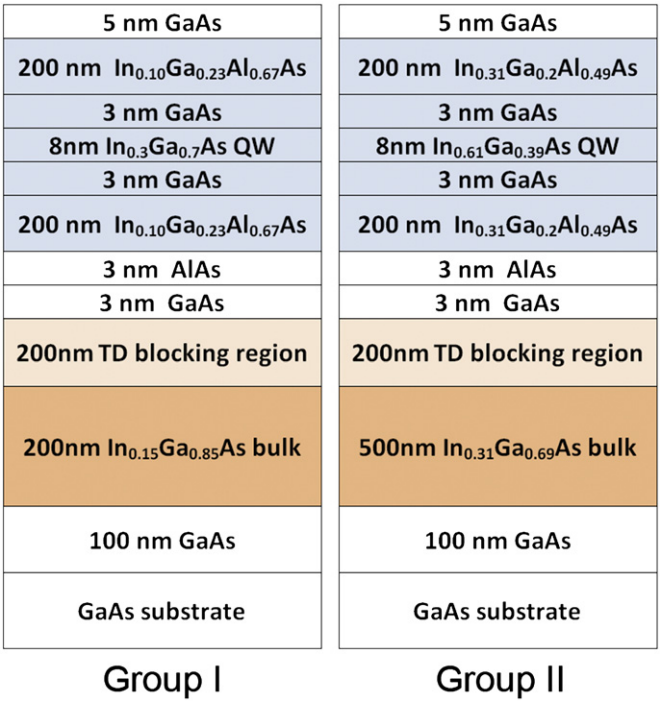

Fig. 1. Schematic structure of the samples. (For interpretation of the references to color in this figure legend, the reader is referred to the web version of this article.)

2.2. Identification of the defect types in QWs

Most of the previous work trying to improve the quality of metamorphic structures mainly focuses on suppression of TDs [20–22]. Since the structure of the QWs is identical in all the samples within the same group, it is reasonable that they have very similar properties regarding to the point defects and other non-radiative recombination centers. The QW grown on the metamorphic template is fully strained and there are no misfit dislocations in the QW. Misfit dislocations are only found at the interface between the relaxed buffer layer and the GaAs buffer layer by TEM. The TDs come from the lattice mismatched interface below the QW structure and should be the only defects affected by the "TD blocking region". In order to confirm this deduction, temperature-dependent PL measurements were carried out for the Ref and N1 samples shown in Fig. 2. The two curves are quite similar and no evidence of localized states is observed at low temperatures within the precision of the measurement. The difference of the bandgap energies between the two samples is caused by different residual strain in the QWs.

2.3. Indication method of TD density

TEM has been performed in 100 nm thick species with a scan range of 10 μm. No obvious TDs in the QW region are observed in the Ref and other samples, indicating a low initial TD density in 10^7 cm^{-2} or lower. TEM images of Ref and S2 samples are shown in Fig. 3 as examples. The QW and all other interfaces are very smooth confirming the 2D growth nature. Misfit dislocations (MDs) are observed at GaAs/$In_{0.15}Ga_{0.85}As$ interface but few TDs are found in the image. For such a low TD density, TEM is not capable of comparing the TD densities and it was very difficult to directly reveal TD blocking events. The inset of Fig. 3b shows a seemingly short section of TD stopped at the $GaN_{0.012}As_{0.988}/In_{0.3}Al_{0.7}As$ SL. The AFM (not shown here) reveals a typical cross-hatch pattern for all the samples with a root-mean-square roughness value of about 2 nm from a scan area of 10×10 μm^2. The textured surface pattern prohibits using sensitive etching methods to count the etch pity

Table 1
Detail structures of the "TD blocking region" and the relative PL intensity of Group I and II samples. The PL intensity is scaled to the reference sample (Ref and II-Ref) within each group.

Label	Structure of the "TD blocking region"	Relative PL intensity (a.u.)
Group I		
Ref	200 nm bulk $In_{0.15}Ga_{0.85}As$	100
N1	(5 nm $In_{0.15}Ga_{0.85}As$+5 nm $In_{0.15}Ga_{0.85}N_{0.012}As$) × 20 periods	312
N2	(5 nm $In_{0.15}Ga_{0.85}As$+5 nm $In_{0.15}Ga_{0.85}N_{0.019}As$) × 20 periods	226
N3	(5 nm $In_{0.15}Ga_{0.85}As$+5 nm $In_{0.15}Ga_{0.85}N_{0.024}As$) × 20 periods	220
S1	(5 nm GaAs+5 nm $In_{0.3}Al_{0.7}As$) × 20 periods	254
S2	(5 nm $GaN_{0.012}As_{0.988}$+5 nm $In_{0.3}Al_{0.7}As$) × 20 periods	426
S3	(5 nm GaAs+5 nm $In_{0.3}Al_{0.7}N_{0.012}As_{0.988}$) × 20 periods	370
S4	(5 nm $GaN_{0.012}As_{0.988}$+5 nm $In_{0.3}Al_{0.7}N_{0.012}As_{0.988}$) × 20 periods	465
S5	(5 nm GaAs+5 nm $In_{0.336}Al_{0.664}N_{0.012}As_{0.988}$) × 20 periods	434
A1	(5 nm AlAs+5 nm $In_{0.3}Al_{0.7}As$) × 20 periods	128
A2	(5 nm AlAs+5 nm $In_{0.3}Al_{0.7}N_{0.012}As_{0.988}$) × 20 periods	435
Group II		
II-Ref	700 nm bulk $In_{0.31}Ga_{0.69}As$	100
II-N	(5 nm $In_{0.31}Ga_{0.69}As$+5 nm $In_{0.31}Ga_{0.69}N_{0.012}As$) × 20 periods	193

density that directly links to the number of TDs. For these reasons, PL is chosen as the main tool to assess material quality below.

Photo-excited carriers in the PL measurements will recombine non-radiatively at dislocations at a rate of ps as compared with a typical radiative lifetime of ns. As they can diffuse in QWs for a long distance up to micrometers, they are very sensitive to the TDs. Below we give a simple estimation showing that PL is a sensitive tool for TD density in the range of 10^5–10^7 cm^{-2}. If we assume that TDs are uniformly distributed with a density of n and the lateral carrier diffusion length of d, then for a unit area of the QW, a proportion

$$R = n\pi d^2 \quad (1)$$

will generate no light. When $R \geq 1$, there will be no PL signal. We have previously measured such a diffusion length from GaInNAs QWs emitting at 1.3 μm using scanning near-field optical microscopy (SNOM) and found that the diffusion coefficient was about 25 cm^2/s [23]. If we assume that the radiative recombination time is 1 ns, which is typical in InGaAs QWs, the lateral diffusion length d is about 1.6 μm. From Eq. (1) the R-value is about 0.01 for $n=10^5$ cm^{-2} and increases to 1 when $n=10^7$ cm^{-2}. In a real sample, the TDs are non-uniformly distributed and the R-value is thus smaller than that estimated from Eq. (1). Therefore, PL is a suitable indirect tool to assess the TD density in the range of 10^5–10^7 cm^{-3}.

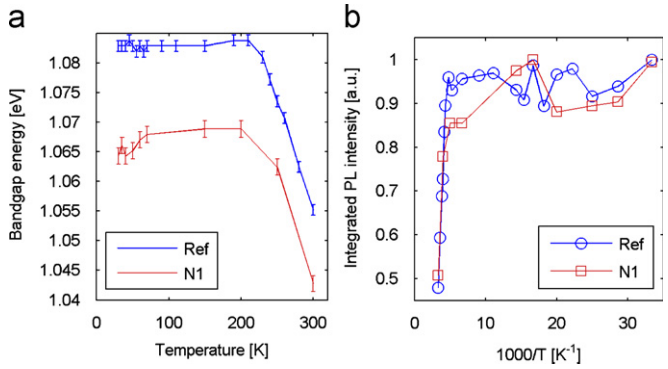

Fig. 2. Temperature-dependent PL measurements: (a) transition energy vs temperature and (b) integrated PL intensity vs temperature.

3. Results and discussions

3.1. Group I samples

It should be noticed from the structure of Group I samples that the In composition in the barriers surrounding the QW is 10%, which is 5% less than that in the relaxed buffer and the TD blocking region. This is due to the so-called "setback" problem [24], as the 200 nm thick $In_{0.15}Ga_{0.85}As$ buffer grown on GaAs is not fully relaxed. Therefore, a reduced In composition in the following structure is required to match the lateral lattice constant and avoid formation of new MDs above the TD blocking region. The validity of the chosen value is confirmed by the (1 1 5) and the (1 1 $\bar{5}$) rocking curves of XRD measurements. The measured relaxation rate is 95 and 100% for the $In_{0.15}Ga_{0.85}As$ buffer and the $In_{0.1}Ga_{0.23}Al_{0.67}As$ layer in the Ref sample, respectively, which means the barrier is fully relaxed without any residual strain.

For sample N1, the nitrogen source was turned on and off after each 5 nm growth of $In_{0.15}Ga_{0.85}As$ resulting in an $In_{0.15}Ga_{0.85}As$/$In_{0.15}Ga_{0.85}N_{0.012}As_{0.988}$ SL. It is similar for N2 and N3 samples but with higher N concentrations. The concentration of incorporated N is extracted by fitting the XRD (0 0 4) rocking curves, in which the III-N components are treated as zincblende crystal structures. The resulted N concentrations are 1.2, 1.9 and 2.4% for N1, N2 and N3, respectively. Fig. 4 shows PL spectra of the three N-samples together with the Ref. We can find that incorporation of N dramatically enhances the PL intensity with a maximum of 3.7 times indicating a strong TD blocking effect from the nitrogen. However, further increase in the N concentration leads to a slight drop in the PL intensity but still better than the reference sample. This suggests that there might exist an optimized N concentration for the TD blocking effect.

Fig. 5 shows a comparison of the XRD (0 0 4) rocking curves of Ref and N1 with the main features labeled. The SL structure gives rise to diffraction peaks in the rocking curve. The clearest one is the 1st order peak while the 0th order peak lies between the two layer peaks making it difficult from being distinguished. The thickness of one period of the SL can be obtained by measuring the separation of

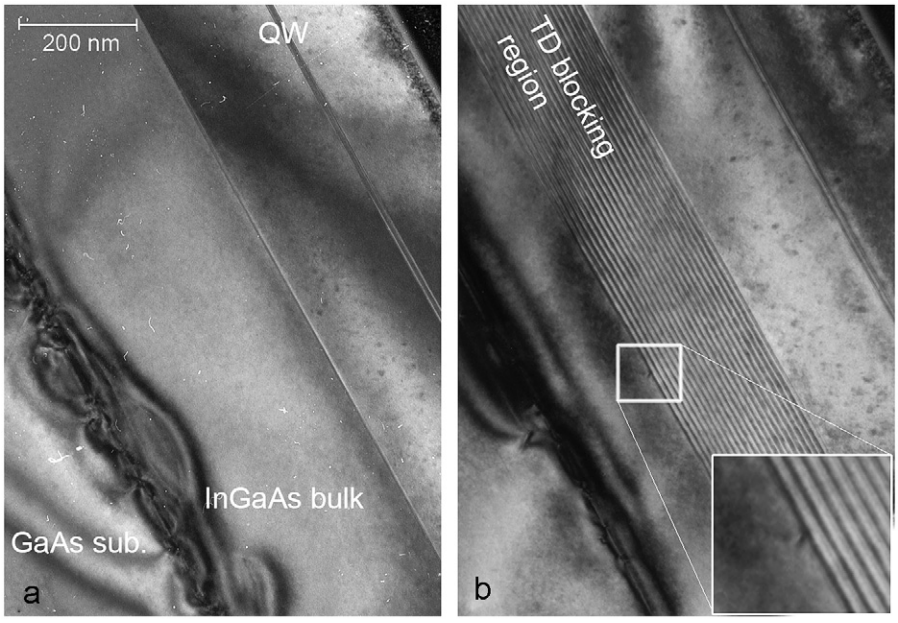

Fig. 3. Cross-section TEM images of sample (a) Ref and (b) S2. The inset in (b) shows a seemingly TD segment stopped at the SL.

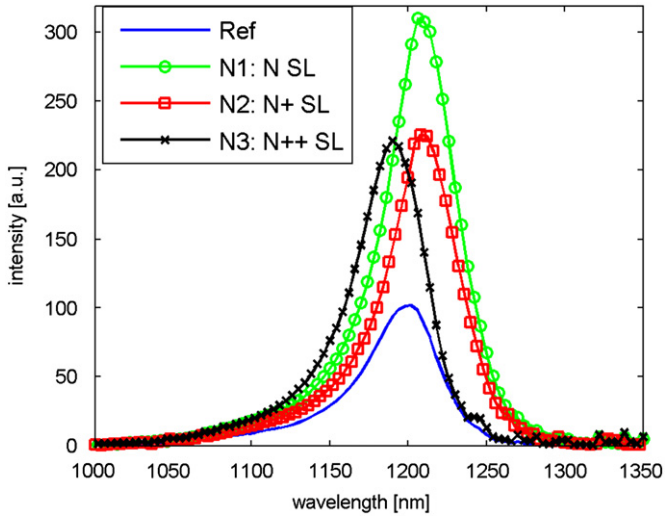

Fig. 4. PL spectra of the samples Ref, N1, N2 and N3.

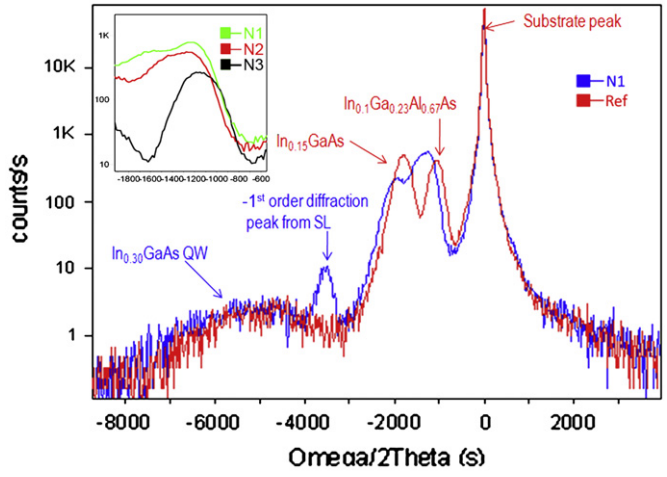

Fig. 5. XRD (0 0 4) rocking curves of the samples Ref and N1. The inset shows the relative positions of the $In_{0.1}Ga_{0.23}Al_{0.67}As$ peak of samples N1, N2 and N3.

the diffraction peaks and is 9.28, 8.98 and 8.95 nm for N1, N2 and N3, respectively. As we know from the discussions above, the $In_{0.1}Ga_{0.23}Al_{0.67}As$ layers in the Ref sample are fully relaxed. If we compare the $In_{0.1}Ga_{0.23}Al_{0.67}As$ peak of sample N1 with that of sample Ref, the peak of sample N1 is shifted to a lower angle value. This indicates the existence of residual strain in the $In_{0.1}Ga_{0.23}Al_{0.67}As$ barrier of the QW. The "setback" value is optimized for the Ref sample. Incorporation of N in the "TD blocking region" breaks this matching and results in residual strain in the QW structure. Higher N concentration is expected to cause more residual strain and move the $In_{0.1}Ga_{0.23}Al_{0.67}As$ peak further to lower angle value in XRD rocking curve. However, this is not the case if we compare the $In_{0.1}Ga_{0.23}Al_{0.67}As$ peaks of sample N1, N2 and N3 in the inset of Fig. 5. The peak of N2 is indeed a little to the left of that of N1, but that of N3 is to the right. This inconsistency suggests new strain relaxation in the QW structure, which moves the $In_{0.1}Ga_{0.23}Al_{0.67}As$ peak to larger angle value. It seems that for N2 only very small amount of strain is relaxed so the $In_{0.1}Ga_{0.23}Al_{0.67}As$ peak is still to the left of that of N1. For N3, more residual strain leads to more strain relaxation moving the peak to the right side of N1. Despite all this, the $In_{0.1}Ga_{0.23}Al_{0.67}As$ layers in N3 are still more strained than that of the Ref sample (not shown in the figure). This new strain relaxation could explain why higher N concentration leads to lower PL intensity. It is possible to enhance the TD blocking effect by using high nitrogen composition if the "setback" is optimized for each different nitrogen composition.

There are two sources that have an effect on dislocation dynamics when incorporating N: the tensile strain caused by the small covalent radius of N and the lattice hardening effect due to high bond strengths of N with group-III atoms [25]. In order to further investigate both effects, we incorporate N into different parts of a strain compensated GaAs/$In_{0.3}Al_{0.7}As$ SL (the S-series samples shown in Table 1). The GaAs layers in the SL are tensile strained while the $In_{0.3}Al_{0.7}As$ layers are compressively strained when grown on an $In_{0.15}Ga_{0.85}As$ buffer. The average strain of the SL is matched to the $In_{0.15}Ga_{0.85}As$ buffer. The PL intensities of these samples are summarized in Table 1. As discussed in [19], comparison of the PL intensities from the S-samples evidences that strain accounts for at least part of the reasons of the dislocation blocking effect while the lattice hardening effect is the dominating mechanism. The sample S5 was designed to dispel the strain effect by using a slightly higher In of 33.6% to compensate the tensile strain of 1.2% N. The PL intensity is improved by 70% as compared to S1, which confirms the impact of the lattice hardening effect.

The lattice hardening effect has also been observed in other materials, for example, when GaAs is highly doped by Si [26] and the alloy of AlGaAs [27] or InAlAs [28] with high Al concentrations. This effect was evidenced by hindering the formation and motion of MDs as a result of the enhanced bonding strength leading to an increased critical thickness [25,26]. The same impact could also make it difficult for the TDs to thread through the hard material and forces them to be bent [27]. Two more samples A1 and A2 were designed similar to S1 and S3 but with GaAs replaced by AlAs because AlAs is harder than GaAs. The PL results are summarized in Table 1 and Fig. 6. It is found that, without N, the A1 has lower PL intensity than S1 probably due to the inferior AlAs structural quality and rough interface when grown at a relatively low temperature (500 °C). However, when N is incorporated, the improvement in PL intensity is stronger for sample A2 than S3. This gives again evidence that the lattice hardening effect contributes to the TD blocking effect.

3.2. Group II samples

In order to reach 1.55 μm emissions, the In composition of the buffer layer and the barrier of the QW is increased to 31% and that of the QW layer is increased to 61%. Two samples: II-REF and II-N,

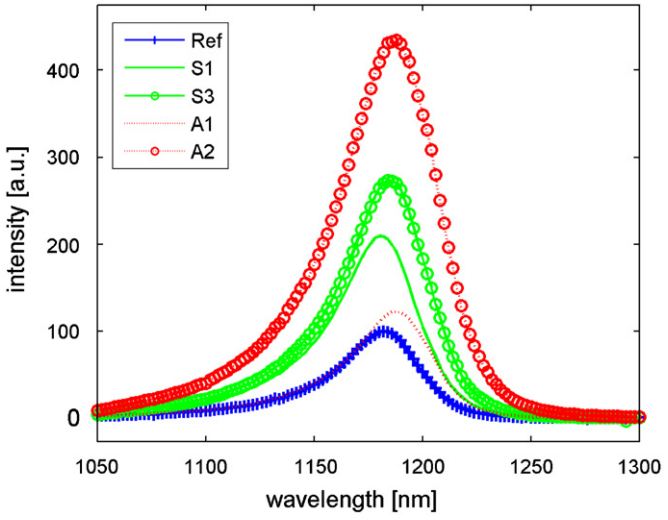

Fig. 6. PL spectra of the samples Ref, S1, S3, A1 and A2.

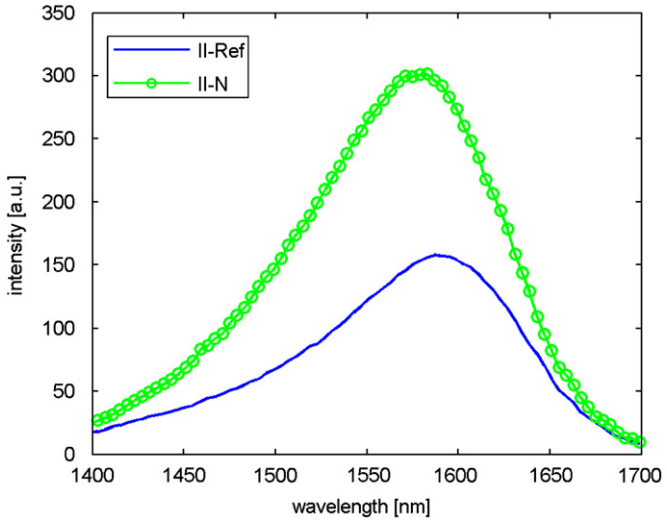

Fig. 7. PL spectra of the samples II-Ref and II-N.

were grown with the structures shown in Fig. 1 and Table 1. Because the relaxed buffer layer is much thicker in this case, it is believed that the strain is almost fully relaxed, so no In composition setback is designed here. The PL spectra are shown in Fig. 7. The wavelength of both samples is around 1.55 to 1.58 μm, respectively, while the peaks are very broad indicating low structural quality. The PL intensity of the II-N sample shows two times improvement in PL intensity, which is less effective than those of the group I samples (S1 and S2). We believe that it could be related to the different types of TDs under different mismatch conditions. For small lattice mismatched metamorphic buffers, most of the TDs are of 60° type, which are easy to glide and bend. While in the large lattice mismatched case, the TDs can be a mixture of both 60° and 90° type or even only 90° type. These 90° type TDs are very difficult to be bent or blocked. Therefore, it is likely that the incorporated N can have an effect only on 60° TDs and the improvement is limited. Combination of N incorporation and strained compensated SL ($In_{0.41}Al_{0.59}As/In_{0.21}Ga_{0.48}Al_{0.31}As$) was also tested. However, no improvement of PL intensity was obtained. The probable reason can be that the SL with a very high In composition is partially relaxed due to the compositional non-uniformity, which would lead to large local lattice mismatch.

4. Conclusions

Strong enhancement of PL intensity from metamorphic InGaAs QWs by incorporating N in buffers grown on GaAs substrates was demonstrated and investigated. A 3.7 or 5.4 times improvement of PL intensity from the QWs can be obtained when using a dilute N SL alone or combining dilute N incorporation with a strain compensated $GaAs/In_{0.3}Al_{0.7}As$ SL, respectively. The enhancement of PL intensity indicates a strong TD blocking effect by the incorporated N. Two mechanisms are identified for the PL improvement: the weak strain effect and the strong lattice hardening effect. The improvement is less effective for highly lattice matched buffers, presumably due to the presence of immobile 90° type TDs.

Acknowledgement

The Swedish Research Council (VR) is acknowledged for financial support for this project.

References

[1] N. Rorsman, C. Karlsson, S.M. Wang, H. Zirath, T.G. Andersson, Electron. Lett. 31 (1995) 1292.
[2] W.E. Hoke, R.E. Leoni, C.S. Whelan, T.D. Kennedy, A. Torabi, P.F. Marsh, Y. Zhang, C. Xu, K.C. Hsieh, J. Vac. Sci. Technol. B 22 (2004) 1554.
[3] S.M. Wang, I. Tangring, Q.F. Gu, M. Sadeghi, A. Larsson, X.D. Wang, C.H. Ma, I.A. Buyanova, W.M. Chen, Thin Solid Films 515 (2006) 4348.
[4] M. Sugo, H. Mori, Y. Sakai, Y. Itoh, Appl. Phys. Lett. 60 (1992) 472.
[5] M. Arai, T. Tadokoro, T. Fujisawa, W. Kobayashi, K. Nakashima, M. Yuda, Y. Kondo, Electron. Lett. 45 (2009) 359.
[6] J. Chen, J.M. Fernández, J.C.P. Chang, K.L. Kavanagh, H.H. Wieder, Semicond. Sci. Technol. 7 (1992) 601.
[7] D. Lubyshev, J.M. Fastenau, X.-M. Fang, Y. Wu, C. Doss, A. Snyder, W.K. Liu, M.S.M. Lamb, S. Bals, C. Song, J. Vac. Sci. Technol. B 22 (2004) 1565.
[8] S.I. Molina, F.J. Pacheco, D. Araujo, R. Garcia, A. Sacedon, E. Calleja, Z. Yang, P. Kidd, Appl. Phys. Lett. 65 (1994) 2460.
[9] S.M. Wang, C. Karlsson, N. Rorsman, M. Bergh, E. Olsson, T.G. Andersson, H. Zirath, J. Cryst. Growth 175/176 (1997) 1016.
[10] I. Tångring, H.Q. Ni, B.P. Wu, D.H. Wu, Y.H. Xiong, S.S. Huang, Z.C. Niu, S.M. Wang, Z.H. Lai, A. Larsson, Appl. Phys. Lett. 91 (2007) 221101.
[11] K.E. Lee, E.A. Fitzgerald, J. Cryst. Growth 312 (2010) 250.
[12] I.J. Fritz, P.L. Gourley, L.R. Dawson, J.E. Schirber, Appl. Phys. Lett. 53 (1988) 1098.
[13] Z. Mi, J. Yang, P. Bhattacharya, D.L. Huffaker, Electron. Lett. 42 (2006) 121.
[14] I. Tangring, S.M. Wang, M. Sadeghi, A. Larsson, Electron. Lett. 42 (2006) 691.
[15] D. Wu, H. Wang, B. Wu, H. Ni, S. Huang, Y. Xiong, P. Wang, Q. Han, Z. Niu, I. Tangring, S.M. Wang, Electron. Lett. 44 (2008) 474.
[16] Y.Q. Wei, J.S. Gustavsson, M. Sadeghi, S.M. Wang, A. Larsson, Opt. Express 14 (2006) 2753.
[17] J.S. Gustavsson, Y.Q. Wei, M. Sadeghi, S.M. Wang, A. Larsson, Electron. Lett. 42 (2006) 925.
[18] J. Schone, E. Spiecker, F. Dimroth, A.W. Bett, W. Jager, Appl. Phys. Lett. 92 (2008) 081905.
[19] Y.X. Song, S.M. Wang, Z.H. Lai, M. Sadeghi, Appl. Phys. Lett. 97 (2010) 091903.
[20] I. Tangring, S.M. Wang, X.R. Zhu, A. Larsson, Z.H. Lai, M.A. Sadeghi, Appl. Phys. Lett. 90 (2007) 071904.
[21] H. Choi, Y. Jeong, J. Cho, M.H. Jeon, J. Cryst. Growth 311 (2009) 1091.
[22] Y.X. Song, S.M. Wang, I. Tangring, Z.H. Lai, M. Sadeghi, J. Appl. Phys. 106 (2009) 123531.
[23] G. Adolfsson, S.M. Wang, M. Sadeghi, J. Bengtsson, A. Larsson, J.J. Lim, V. Vilokkinen, P. Melanen, IEEE Photon. Technol. Lett. 21 (2009) 134.
[24] J. Tersoff, Appl. Phys. Lett. 62 (1993) 693.
[25] K. Momose, H. Yonezu, Y. Fujimoto, K. Ojima, Y. Furukawa, A. Utsumi, K. Aiki, Jpn. J. Appl. Phys. 41 (2002) 7301.
[26] B.K. Tanner, P.J. Parbrook, C.R. Whitehouse, A.M. Keir, A.D. Johnson, J. Jones, D. Wallis, L.M. Smith, B. Lunn, J.H.C. Hogg, Appl. Phys. Lett. 77 (2000) 2156.
[27] N. Hayafuji, S. Ochi, M. Miyashita, M. Tsugami, T. Murotani, A. Kawagishi, J. Cryst. Growth 93 (1988) 494.
[28] Y. Jeong, M. Shindo, H. Takita, M. Akabori, T. Suzuki, Phys. Status Solidi (c) 5 (2008) 2787.